Magnetic Field Enhanced Coherence Length in Cold Atomic Gases

Olivier Sigwarth, Guillaume Labeyrie, Thibaut Jonckheere, Dominique Delande, Robin Kaiser, Christian Miniatura

Increasing coherent backscattering with a magnetic field

O. Sigwarth,[1,*] G. Labeyrie,[2] T. Jonckheere,[1,†] D. Delande,[1] R. Kaiser,[2] and C. Miniatura[2]

[1] *Laboratoire Kastler Brossel, Tour 12, Etage 1, 4 Place Jussieu, F-75005 Paris, France*
[2] *Institut Non Linéaire de Nice, 1361 route des Lucioles, F-06560 Valbonne, France.*

(Dated: January 23, 2004)

We study the effect of an external magnetic field on coherent backscattering (CBS) of light from a laser-cooled rubidium vapor. We observe that the CBS enhancement factor can be *increased* with B, in sharp contrast with usual scatterers. This surprising behavior is mainly due to the lifting of the degeneracy in the ground state of the rubidium atom. We find good agreement between our experimental data and a full Monte-Carlo simulation, taking into account the magneto-optical effects and the geometry of the atomic cloud.

PACS numbers: 42.25.Dd, 33.55.Ad, 32.80.Pj

Coherent backscattering is a spectacular manifestation of the interference phenomena occuring when a wave propagates inside a random scattering medium [1, 2]. It consists in an enhancement of the diffuse intensity in the backward direction, due to the interference between reversed scattering paths, visiting the same scatterers in reverse order. The interference is constructive in the exact backscattering direction, and, after configuration averaging, the intensity profile is cone shaped, with an angular width of order $1/(k\ell^*) \ll 1$ where k is the wavevector and ℓ^* the transport mean free path. The enhancement is maximal when the amplitudes of the reversed paths are exactly balanced. For time-reversal symmetric systems, the interfering amplitudes are equal for a convenient choice of the polarization channel, and an enhancement factor close to 2 is observed [2]. Adding an external magnetic field breaks the time-reversal symmetry, leading to unbalanced interfering amplitudes and consequently to a *decrease* of the enhancement factor [3, 4]. In this letter, we report the first study of CBS on a cold atomic vapor in an external magnetic field B, showing an a priori surprising *increase* of the enhancement factor with B. The reason for this unexpected result is the existence of an internal structure of the atoms (a non-zero angular momentum, hence degenerate, ground state) which is already responsible, at zero magnetic field, for unbalanced interfering amplitudes and reduced enhancement factor [5, 6, 7]. The magnetic field breaks the degeneracy of the atomic ground state (Zeeman effect), and splits the atomic resonance line. At large enough B, only a few Zeeman sublevels effectively participate in the multiple scattering process, thus partly restoring the large enhancement factor characteristic of non-degenerate scatterers. The paper is organized as follows. We first briefly describe the experiment. We then discuss the basic physical ingredients and the principle of the Monte-Carlo simulation. Then, we compare the results of the simulations to the experimental data and identify the various mechanisms at work, trying to give some simple physical pictures.

The experimental setup to produce the optically-thick cloud of cold atoms and to record the CBS signal has been described in [5]. In addition to the usual setup, we added a pair of coils in the Helmholtz configuration to produce the external magnetic field. The experimental geometry is described in Fig. 1. A probe laser beam of diameter 11 mm and homogenous intensity (total power 0.1 mW, saturation parameter at zero magnetic field: 0.03), with wavevector $\mathbf{k}$ and circular polarization $\boldsymbol{\epsilon}$, is shined at the atomic cloud during 400 μs while the magneto-optical trap (MOT) is off. This CBS laser is quasi-resonant with the $F = 3 \rightarrow F' = 4$ transition of the D2 line of Rb^{85} (wavelength λ = 780nm, linewidth $\Gamma/2\pi$ = 5.9 MHz). During the CBS measurements, the laser is tuned to resonance with the $m_F = 3 \rightarrow m_{F'} = 4$ transition (quantization axis along $\mathbf{B}$). The MOT sequence (total duration 20 ms), includes a molasse sequence of 1 ms to further cool the cloud (typical rms velocity 0.1 m/s). Before the CBS probe is applied, we switch on the current in the extra pair of coils to create a magnetic field $\mathbf{B}$ orthogonal to $\mathbf{k}$. The CBS cone is recorded in the so-called parallel helicity channel, where the detected helicity is identical to the incident one. A mechanical chopper, synchronized with the time sequence, blocks all light when the MOT is on. The whole cycle is repeated several thousand times to obtain one CBS peak. Results are shown in Fig. 2, where the enhancement factor α is plotted as a function of B. It is observed that α, initially very small (≈ 1.05 for B=0), sharply increases with B to saturate around 1.33 above 30G. This behavior is obviously very different from the classical case [4], where α is reduced by the presence of B in all instances.

The diffuse light intensity radiated by an optically-thick sample can be seen as resulting from the interference of many "partial waves" scattered along all possible paths in the medium. A multiple scattering path can be decomposed in a succession of N (N is the scattering order) elementary steps, each involving two consecutive events : the scattering by a particle followed by the propagation in an effective medium until the next scattering event. When a magnetic field $\mathbf{B}$ is applied, the atomic energy levels are shifted by an amount $\Delta E = gm\mu B\hbar$,

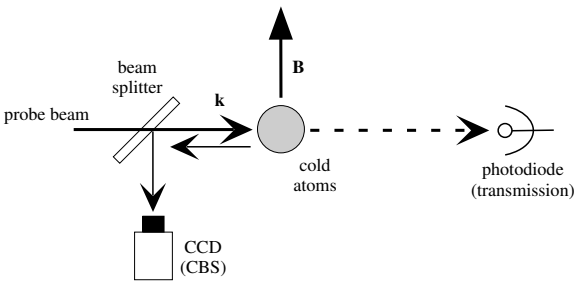

FIG. 1: Principle of the experiment. An external magnetic field **B** is applied orthogonally to the incident wavevector **k**. A circularly-polarized laser beam is shined at the cold atomic cloud, and the backscattered far-field intensity distribution is recorded on a CCD (detection in the parallel helicity channel). The coherent transmission through the cloud center is also monitored.

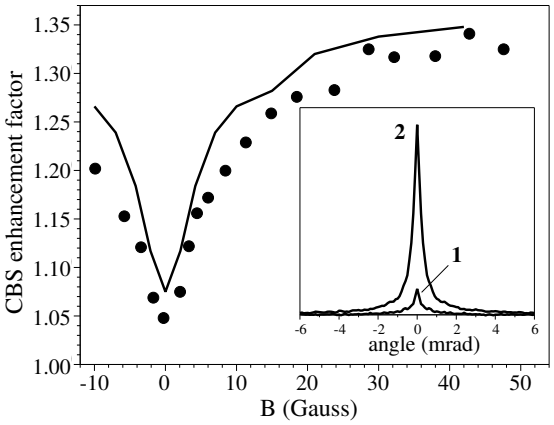

FIG. 2: CBS enhancement factor of light on a cold Rb atomic cloud, measured in the parallel helicity channel $h \parallel h$, as a function of the transverse magnetic field B (circles); it shows a dramatic *increase* at non-zero magnetic field when time-reversal symmetry is broken. For each B value, the laser is tuned to resonance with the $m_F = 3 \rightarrow m_{F'} = 4$ transition. The solid line is the result of the Monte-Carlo simulation (no adjustable parameter). The inset shows two experimental profiles of CBS peaks (angular averages) for B=0 (1) and B=43G (2).

where g is the Landé factor (respectively 1/3 and 1/2 for the ground and excited state considered here), m the magnetic quantum number and $\mu/2\pi = 1.4$ MHz/G the Zeeman shift rate. The Zeeman splitting into a non-degenerate structure affects both the properties of an individual scatterer and of the effective medium. The total scattering, as well as the differential cross-section (radiation pattern) are modified [8]. An essential difference between a usual scatterer and an atom is that the atom has an extremely resonant scattering cross-section (quality factor of the order of 10^8), so that few Gauss are enough to induce a Zeeman shift comparable to the resonance linewidth, and consequently a large modification of the scattering cross-section. This is also why the CBS enhancement factor displays dramatic changes, even at moderate B, in sharp contrast with published experimental results on standard scatterers which require magnetic fields of several teslas [4]. An additional complication with atoms is the existence of several Zeeman sublevels, so that a change in the Zeeman sublevel during the scattering event leads to inelastic Raman scattering. Provided a single closed $F \rightarrow F'$ transition is close to resonance with the incident laser beam, the scattering amplitude of an incident photon $|\mathbf{k}\boldsymbol{\epsilon}\rangle$ onto the outgoing light state $|\mathbf{k'}\boldsymbol{\epsilon'}\rangle$ by an atom whose initial state $|Fm_1\rangle$ is changed to $|Fm_2\rangle$ is described by the scattering matrix T_{m_1,m_2}:

$$\overline{\boldsymbol{\epsilon'}}.T_{m_1,m_2}.\boldsymbol{\epsilon} = \sum_{m'=-F'}^{F'} \frac{\langle Fm_2|\mathbf{d}.\overline{\boldsymbol{\epsilon'}}|F'm'\rangle\langle F'm'|\mathbf{d}.\boldsymbol{\epsilon}|Fm_1\rangle}{\delta + \mu B(gm_1 - g'm') + i\Gamma/2} \quad (1)$$

where $\mathbf{d}$ is the atomic dipole operator and $\delta = \omega - \omega_0$ is the detuning of the laser frequency ω from the zero-field atomic frequency ω_0. The scattered photon has a frequency $\omega' = \omega + g\mu B(m_1 - m_2)$ and polarization $\Delta_{\mathbf{k}'} T_{m_1,m_2} \boldsymbol{\epsilon}$, where $\Delta_{\mathbf{k}'}$ is the projector on the plane perpendicular to $\mathbf{k}'$.

The effective medium is characterized by its complex refractive index, whose imaginary part describes the attenuation of the wave as it propagates, i.e. mean-free path ℓ. The effect of a magnetic field on the effective medium is well documented [3, 9]: a polarization propagating along a given direction decomposes on two eigenmodes which propagate with a relative change of phase (Faraday effect) and differential attenuation (Cotton-Mouton effect). Because of magnetically induced birefringency, we have to distinguish the electric field from the electric induction. The later induces the atomic dipole and is the variable of interest. In the case of a uniform density medium, the propagation of the electric induction inside the effective medium is described by the Green function:

$$G(\mathbf{r}, \omega) = -\frac{\omega}{2\pi r} e^{ikrN(\omega)} \Delta_{\mathbf{r}} \quad (2)$$

where $N(\omega) = 1 - \Sigma(\omega)/k$ is the refractive index matrix. For low densities, the self-energy $\Sigma(\omega)$ is given by the Boltzmann approximation: $\Sigma = n\langle T\rangle$ with n the uniform density of scatterers and $\langle T\rangle$ the scattering matrix averaged over the internal degrees of freedom. Important assumptions are made to calculate $\langle T\rangle$: all Zeeman sub-states are assumed to be equally populated, which is a good approximation for atoms produced in the MOT, and optical pumping is neglected. As explained below, this assumption is likely to be correct if the incident light is resonant with the $m_F = 3 \rightarrow m_{F'} = 4$ transition, like

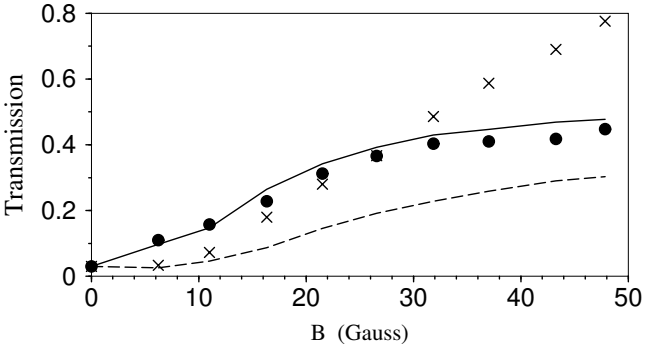

FIG. 3: We plot the measured coherent transmission (normalized to the incident intensity) through the cloud center as a function of the magnetic field B. The filled circles correspond to light tuned to resonance with the $m_F = 3 \rightarrow m_{F'} = 4$ transition, detuned from the zero-field resonance by $\delta = \mu B$, while the crosses are obtained at $\delta = 0$. The solid and dashed lines are the corresponding curves obtained with Monte-Carlo simulations. See text for interpretation.

in our experiment. Under these two assumptions:

$$\langle T \rangle = \frac{1}{\delta + i\Gamma/2} \mathbf{\Delta_k} \begin{pmatrix} \zeta & \eta & 0 \\ -\eta & \zeta & 0 \\ 0 & 0 & \zeta + \theta \end{pmatrix} \mathbf{\Delta_k} \qquad (3)$$

where ζ, η and θ are simple functions of $\phi = \frac{i\mu B}{\delta + i\Gamma/2}$ whose detailed expressions will be published elsewhere. ζ describes the normal extinction of the light in the medium, while η and θ respectively describe the Faraday rotation and the Cotton-Mouton effect. The scattering matrix (1) and the Green function (2) are the basic ingredients of the physics taking place in the medium. They are used in a Monte-Carlo simulation, where the photons are randomly launched in the medium, and their contributions to the diffuse intensity properly collected. The details – especially, how to take into account the non-uniform atomic density in the atomic cloud – are described in [6]. The amplitudes of the direct and reversed paths are calculated, giving a contribution to the corresponding scattering order for the incoherent intensity $|a_{\rm dir}|^2 + |a_{\rm rev}|^2$ and the interference term, also called coherent intensity, $2\Re\left(a_{\rm dir}\overline{a_{\rm rev}}\right)$. Single scattering paths are an exception, as the direct and reversed paths then coincide, and the interference term does not exist. $I_{\rm single} + I_{\rm inc}$ is the average (after configuration averaging) diffusive intensity, while $I_{\rm coh}$ describes the CBS cone. The enhancement factor at exact backscattering is thus obtained as $\alpha = 1 + I_{\rm coh}/(I_{\rm single} + I_{\rm inc})$. To check the validity of our simulations, we also calculate the coherent transmission through the center of the cloud, and compare it to the experimentally measured full transmission of the beam.

Fig. 3 shows how coherent transmission evolves as the magnetic field is varied. The probe beam polarization is circular. The optical thickness at zero **B** field is 31. The filled circles correspond to a laser tuned to the $m_F = 3 \rightarrow m_{F'} = 4$ transition, and the crosses to $\delta = 0$. The solid lines are the results of the Monte-Carlo simulation. In the first case, the agreement is good for all B values. In the second case, the measured transmission is significantly larger than the theoretical one above 10G. This behavior is due to optical pumping: at large B, the few Zeeman sublevels resonant with the laser are efficiently depleted by Raman scattering, yielding an increasing transmission of the medium. On the contrary, for $\delta = \mu B$, the only resonant transition is the *closed* $m_F = 3 \rightarrow m_{F'} = 4$ transition so that $m_F = 3$ cannot be depleted while the other sublevels are not sensitive to the incident light. This interpretation is confirmed by the observation that the transmitted intensity increases in time for $\delta = 0$ (a clear proof that the atomic medium is changing), but does not for $\delta = \mu B$. We thus have convincing indications that optical pumping is negligible in our CBS experiments.

The results of the Monte-Carlo simulations for CBS are shown in Figs. 2 and 4. The calculated enhancement factor is rapidly increasing from $\alpha = 1.07$ at 0 G to $\alpha = 1.35$ at 42 G, in good agreement with the experimental observation. In Fig. 4(a), we plot the ratio of coherent over incoherent intensity as a function of B. At $B = 0$, the coherent intensity is much smaller than the incoherent one. This is due to the amplitude imbalance in the CBS two-paths interference because of the atomic internal structure, see [5]. $I_{\rm coh}/I_{\rm inc}$ increases with B, showing the partial restoration of the interference. As can be seen in Fig. 4(b), this behaviour is due to the increase of the coherent intensity (circles) at small B, and to the strong decrease of the incoherent intensity (crosses). This decrease is related to the decrease of the atomic cross section: the optical thickness is lowered and multiple scattering is reduced. On the contrary, the coherent intensity *increases* at small B, because the reduction of the atomic degeneracy restores the interference. This phenomenon competes with the reduction of multiple scattering: at larger B's, the coherent intensity decreases, but more slowly than the incoherent one.

At large magnetic field, $I_{\rm coh}/I_{\rm inc}$ approaches 1. Indeed, at large B, one can envision the $m_F = 3 \rightarrow m_{F'} = 4$ closed transition as being isolated, yielding an effective two-level system. Under these conditions, the reversed paths have the same amplitudes: the amplitude associated with a scattering path now only depends on its geometry (successive directions of scattering, distance between scatterers) and the incident and detected polarizations. However, the CBS enhancement factor remains noticeably smaller than 2, even at large B, due to single scattering. Indeed, in the effective two-level system, the outgoing polarization is fixed by the resonant transition, and is thus identical for all scattering orders, making it imposssible to discriminate the single and multiple scattering contributions using polarization selection. As can

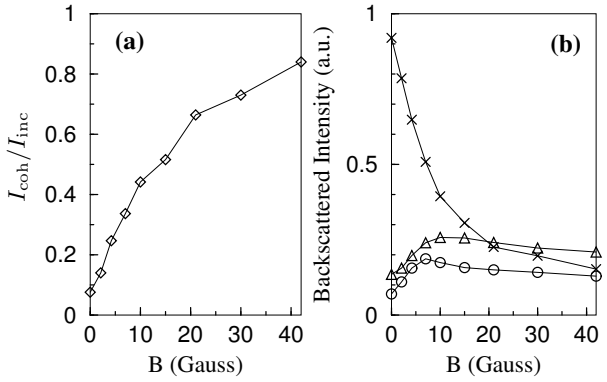

FIG. 4: Results of the Monte-Carlo simulations. (a) shows the increase of the ratio of coherent over incoherent intensity with B. (b) Contribution of single (triangles), incoherent (crosses) and coherent (circles) multiple scattering to the total intensity in the backward direction. Uncertainty on $I_{\rm coh}/I_{\rm inc}$ ranges from 0.01 at 0 G to 0.02 at 42 G. Lines are drawn to guide the eyes.

be seen in Fig. 4(b), $I_{\rm single}$ (triangles) dominates over the other contributions at large B.

The increase of $I_{\rm coh}/I_{\rm inc}$ reveals that the impact of multiple scattering on the CBS cone increases with B. This is illustrated in Table I: at 0 G, double scattering dominates $I_{\rm coh}$ while higher orders contribute significantly to $I_{\rm inc}$. At 30 G, all orders contribute significantly both to $I_{\rm coh}$ and $I_{\rm inc}$. Althought the optical thickness is decreased by **B**, the contribution of multiple scattering to the CBS cone is increased.

We have also studied the impact of magneto-optical effects on the enhancement factor. Monte-Carlo simulations allow to remove them when computing the propagation of the electric induction [10], and to compare the enhancement factors calculated this way to those in Fig. 2. Differences are negligible for $\mu B < \Gamma$ ($\mu B = \Gamma$ corresponds to $B = 4.2$ G in our experiment). For larger values of B, magneto-optical effects show out to lower slightly the enhancememt factor. However, differences remain smaller than 5% at 42 G: magneto-optical effects play no crucial role in the increase of α and can be neglected in a qualitative approach. This situation is very different from the classical one, where Faraday rotation is the key stone to explain the height and shape of the CBS cone.

In conclusion, we have observed a large increase of the CBS enhancement factor in the presence of a magnetic field. This result may seem paradoxical because the magnetic field breaks time-reversal symmetry in classical samples. However, it turns out that the magnetic field splits the degenerate atomic transition into several Zeeman components. At high magnetic field, most of them are out of resonance, leaving an effective two-level system where the two interfering paths have almost equal amplitudes. This restoration of the interference contrast may be a useful tool toward the study of the strong scattering regime with cold atoms.

Scattering order		2	3	4	5
$I_{\rm coh}/I_{\rm inc}$	B=0G	0.21	0.08	0.04	0.02
	B=30G	0.81	0.75	0.69	0.38

TABLE I: Interference contrast for several scattering orders. For each scattering order, we calculate the contribution to the coherent and incoherent intensities. We show the ratio of these contributions for scattering orders ranging from 2 to 5.

We thank CNRS and the PACA Region for financial support. Laboratoire Kastler Brossel is laboratoire de l'Université Pierre et Marie Curie et de l'Ecole Normale Supérieure, UMR 8552 du CNRS.

* Electronic address: sigwarth@spectro.jussieu.fr
† Now at: Centre de Physique Théorique, Campus de Luminy, case 907, 13009 Marseille, France.

[1] D.Y. Sharvin and Y.V. Sharvin JETP Lett. **34**, 272 (1981) ; *Mesoscopic Quantum Physics*, E. Akkermans, G. Montambaux, J.-L. Pichard and J. Zinn-Justin, Eds., Elsevier Science B.V. (North Holland, Amsterdam, 1995).
[2] B. A. van Tiggelen, A. Lagendijk, and A. Tip, J. Phys. Condens. Matter **2**, 7653 (1990); D. S. Wiersma, M. P. van Albada, B. A. van Tiggelen, A. Lagendijk, Phys. Rev. Lett. **74**, 4193 (1995)
[3] F. C. MacKintosh and S. John, Phys. Rev. B **37**, 1884 (1988); A. S. Martinez and R. Maynard, Phys. Rev. B **50**, 3714 (1994); B. A. van Tiggelen, R. Maynard, and T. M. Nieuwenhuizen, Phys. Rev. E **53**, 2881 (1996).
[4] F. A. Erbacher, R. Lenke and G. Maret, Europhys. Lett. **21**, 551 (1993); R. Lenke and G. Maret, Eur. Phys. J. B **17**, 171 (2000); R. Lenke, R. Lehner and G. Maret, Europhys. Lett. **52**, 620 (2000).
[5] G. Labeyrie *et al.* , J. Opt. B: Quantum Semiclass. Opt. **2**, 672 (2000); T. Jonckheere *et al.*, Phys. Rev. Lett. **85**, 4269 (2000)
[6] G. Labeyrie *et al.*, Phys. Rev. A **67**, 033814 (2003)
[7] P. Kulatunga *et al.*, Phys. Rev. A **68**, 033816 (2003)
[8] G. Labeyrie *et al.*, Phys. Rev. Lett. **89**, 163901 (2002)
[9] S. Franke-Arnold, M. Arndt, and A. Zeilinger, J. Phys. B.: At. Mol. Opt. Phys. **34**, 2527 (2001); G. Labeyrie, C. Miniatura and R. Kaiser, Phys. Rev. A **64**, 033402 (2001).
[10] The optical anisotropy of the medium is taken into account to ensure energy conservation: the scattering mean free path depends on the polarization state.